JOURNAL

OF THE AMERICAN CHEMICAL SOCIETY

Registered in U.S. Patent Office. © Copyright, 1981, by the American Chemical Society

VOLUME 103, NUMBER 16 AUGUST 12, 1981

Electronic and Geometric Structural Properties of the Bare Ag_3 Cluster and Ions

Harold Basch

Contribution from the Department of Chemistry, Bar Ilan University, Ramat Gan, Israel.
Received December 12, 1980

Abstract: The electronic and geometric structural properties of Ag_3, Ag_3^-, and Ag_3^+ have been investigated by using an ab initio relativistic effective core potential within the framework of the self-consistent field and configuration interaction methods. For comparison purposes, parallel calculations were also carried out on the silver atom and diatom. Ag_3^- is found to be substantially bound (relative to Ag_3 + an electron) and linear in geometry. On the other hand, Ag_3^+ is calculated to have an equilateral triangular geometry, and a significantly lower ionization potential is predicted for Ag_3 than for Ag_2. The mirror-image, saw-tooth behavior of the electron affinities and ionization potentials of larger silver atom clusters with size, noted in the semiempirical molecular orbital calculations of Baetzold [*J. Chem. Phys.*, **68**, 555 (1978)], is also found here. The ground electronic state of Ag_3 ($^2B_1$) is predicted to be slightly bent with a very shallow bending mode potential surface. At large bend angles (near equilateral triangle geometry), an $^2A_1$ state becomes the ground state, 0.14 eV above the $^2B_1$ state. The $^2A_1$ and $^2B_1$ states are two branches of a Jahn–Teller split degenerate $^2E'$ state at D_{3h} symmetry. The energy proximity of these two states could lead to the geometrical isomerization effects proposed by Ozin et al [*Inorg. Chem.*, **18**, 2932 (1979)] on the basis of low-temperature, rare-gas matrix isolation spectra of Ag_3. The general topological features of the ground-state potential surfaces of Ag_3 and Na_3 [R. L. Martin and E. R. Davidson, *Mol. Phys.*, **35**, 1713 (1978)] are very similar.

The electronic structure description and characterization of small isolated metal atom clusters have been the focus of increasing experimental and theoretical attention for the past several years. Besides the intrinsic interest in them based on their now being experimentally accessible, such clusters have also been proposed as model systems for much larger, more complicated aggregates and polynuclear cluster complexes. The usefulness of the latter approach as detailed, for example, by Muetterties et al.[1] has recently been questioned by Moskovitz.[2] It is now generally believed that isolated small clusters of metal atoms have well-defined electronic and geometric structure properties which are different from the bulk metal[3] and therefore are expected to behave differently in their catalytic properties, which is the main focus of interest in them.

Small silver atom clusters form the latent image in silver halide photography. Because of its presence in, and perhaps stabilization by, ionic crystal lattice substrates, proposed mechanisms for the growth of the latent image typically involve anions or cations of these silver clusters.[4] Bare silver atom clusters and their ions have been investigated theoretically by Baetzold[5,6] mainly with the use of semiempirical molecular orbital methods. Recently, several experimental groups have reported low-temperature, matrix isolation spectroscopy studies of small clusters of silver atoms.[7-9] These latter results typically require a theoretical model or calculated electronic structure for their interpretation. The recent development of practical pseudopotential methods within the framework of ab initio self-consistent field (SCF) theory,[10-12] and their extension to incorporate the dominant relativistic effects into the effective core potential (ECP)[13-16] which replaces the core electrons, now permits the application of ab initio techniques to small silver atom clusters. The electronic structure description obtained thereby can be used to complement the experimental studies by contributing to their understanding. Toward these ends we present here an ab initio relativistic ECP-SCF and configuration interaction (CI) study of the electronic and geometrical structural properties of Ag_n, Ag_n^+, and Ag_n^- (n = 1–3).

Methods and Results

The components of the relativistic core potential which replaces the [Kr] core electrons in the silver atom were generated as described previously for other heavy atoms,[15-17] following the

(1) E. L. Muetterties, T. N. Rhodin, E. Band, C. F. Brucker, and W. R. Pretzer, *Chem. Rev.*, **79**, 91 (1979).
(2) M. Moskovitz, *Acc. Chem. Res.*, **12**, 229 (1979).
(3) H. Basch, M. D. Newton, and J. W. Moskowitz, *J. Chem. Phys.*, **73**, 4492 (1980).
(4) M. R. V. Sahyun, *Photogr. Sci. Eng.* **22**, 317 (1978).
(5) R. C. Baetzold, *J. Chem. Phys.*, **55**, 4355, 4363 (1971).
(6) R. C. Baetzold, *J. Chem. Phys.*, **68**, 555 (1978).
(7) G. Ozin, *Symp. Faraday Soc., No.* **14**, 000 (1980).
(8) W. Schulze and H. Abe, *Symp. Faraday Soc.*, **no. 14**, 87 (1980).
(9) R. Grinter, S. Armstrong, U. A. Jayasooriya, J. McCombie, D. Norris, and J. P. Springall, *Symp. Faraday Soc.*, **no. 14**, 94 (1980).
(10) L. R. Kahn, P. Baybutt, and D. G. Truhlar, *J. Chem. Phys.*, **65**, 3826 (1976).
(11) P. J. Hay, W. R. Wadt, and L. R. Kahn, *J. Chem. Phys.*, **68**, 3059 (1978).
(12) H. Basch, M. D. Newton, J. Jafri, J. W. Moskowitz, and S. Topiol, *J. Chem. Phys.*, **68**, 4005 (1978).
(13) Y. S. Lee, W. C. Ermler, and K. S. Pitzer, *J. Chem. Phys.*, **67**, 5861 (1877).
(14) L. R. Kahn, P. J. Hay, and R. D. Cowan, *J. Chem. Phys.*, **68**, 2386 (1978).
(15) H. Basch and S. Topiol, *J. Chem. Phys.*, **71**, 802 (1979).
(16) H. Basch, D. Cohen, and S. Topiol, *Isr. J. Chem.*, **19**, 233 (1980).
(17) H. Basch, P. S. Julienne, M. Krauss, and M. E. Rosenkrantz, *J. Chem. Phys.*, **73**, 6247 (1980).

0002-7863/81/1503-4657$01.25/0 © 1981 American Chemical Society

Table I. Parameters for the Silver Atom Effective Core Potential

k	n_{kl}	α_{kl}	d_{kl}
		$L = 3^a$	
1	2	0.465542	−0.2966493
2	2	2.03946	−6.396388
3	2	6.80347	−24.37864
4	2	23.8883	−87.59476
5	1	80.8936	−24.07458
6	0	1.20720	−0.0514505
		$l = 2^b$	
1	2	0.365393	−0.2037506
2	2	1.38838	−1.987042
3	2	6.37060	−26.79116
4	2	13.3040	−80.64456
5	2	147.806	193.7982
6	1	7.23407	27.63412
7	0	1.33708	3.040599
		$l = 1^b$	
1	2	0.506868	2.387805
2	2	1.57143	11.60950
3	2	2.59373	12.87600
4	2	33.4897	588.7665
5	2	37.6151	−685.7495
6	1	5.23951	36.10658
7	0	32.0996	1.992041
		$l = 0^b$	
1	2	0.522640	1.952708
2	2	1.76810	16.19212
3	2	5.47390	55.11669
4	2	16.2990	45.69800
5	1	62.0140	42.44565
6	0	0.531320	0.8973770

[a] See eq 2. [b] See eq 3.

methods developed by Kahn et al. for the nonrelativistic case.[10,11] Specifically, the pseudovalence orbitals (PVOs) and corresponding component potentials for $l = 0$ and $l = 2$ were obtained from an all electron relativistic Dirac–Fock (DF) atom SCF calculation for the $[Kr](4d)^4{}_{3/2}(4d)^6{}_{5/2}(5s)^1{}_{1/2}$ ($^2S_{1/2}$) state configuration. The $[Kr](4d)^4{}_{3/2}(4d)^6{}_{5/2}(6p)^1{}_{1/2}$ ($^2P_{1/2}$) and $[Kr](4d)^4{}_{3/2}(4d)^6{}_{5/2}(6p)^1{}_{3/2}$ ($^2P_{3/2}$) state configurations were degeneracy averaged in a single DF atom calculation to give the $l = 1$ PVO and component ECP. The $l = 3$ PVO and component ECP were obtained from averaging the Ag^{10+} $[Kr](4f)^1{}_{5/2}$ ($^2F_{5/2}$) and $[Kr](4f)^1{}_{7/2}$ ($^2F_{7/2}$) state configurations.

The complete atomic core ECP $[U^c(r)]$ is written as

$$U^c(r) = U_L{}^c(r) + \sum_{l=0}^{L-1} \sum_{m_l=-l}^{l} |lm_l> [U_l{}^c(r) - U_L{}^c(r)] < lm_l| \quad (1)$$

with $L = 3$ for the Ag atom. Both $U_L{}^c(r)$ and the difference potentials in brackets above were fitted to analytical functions of the form

$$r^2[U_l{}^c(r) - (N_c/r)] = \sum_k d_{kl} r^{n_{kl}} e^{-\alpha_{kl} r^2} \quad l = L \quad (2)$$

$$r^2[U_l{}^c(r) - U_L{}^c(r)] = \sum_k d_{kl} r^{n_{kl}} e^{-\alpha_{kl} r^2} \quad l < L \quad (3)$$

The resultant parameters of the fit are given in Table I.

For all the component potentials generated here the long-range tails of the numerical ECPs were truncated in the fitting procedure by weighting the region $r > r_{max}$ to force the analytic fit to be very close to zero at $r \approx r_{max}$. These matters, as well as the choice of charged atoms to produce the $l = 3$ component ECP, have been discussed previously.[11,12,16,17] Recently, it has been claimed[18-20] that spurious long-range attractive tails are present in ECPS generated by the general methods of Kahn,[10,11] arising from problems inherent in the long-range behavior of PVOs obtained exclusively by orthogonal transformations of canonical atomic orbitals. Experience has shown[16,21] that the type ECPs generated here are generally not overly attractive in the valence region due to the truncation procedure described above.

Table II. Valence Electron Silver Atom Gaussian Basis Set

orbital	exponent	coeff
4d	52.97	−0.002 223 4
	4.651	0.138 174 5
	1.802	0.425 276 2
	0.6631	0.460 718 6
	0.2162	0.232 032 7
5s	0.9776	−0.210 539 1
	0.08735	1.066 921 3
	0.02357	1.0
5p	0.1200	1.0
	0.03000	1.0

Table III. Calculated and Experimental Atomic State Energies[a]

species	state configuration	all electron[b,c]	valence electron[d]	exptl[e,c]
Ag	$[Kr](4d)^{10}(5s)^1$ (^2S)	0	0	0
	$[Kr](4d)^{10}(5p)^1$ (^2P)	3.06	3.14	3.74
	$[Kr](4d)^9(5s)^2$ (^2D)	3.87	5.03	3.96
Ag^+	$[Kr](4d)^{10}$ (^1S)	6.34	6.43	7.58
Ag^-	$[Kr](4d)^{10}(5s)^2$ (^1S)			−1.30[g]
SCF			0.12	
MCSCF(5)[f]			−0.58	
CI			−0.58	

[a] Energies in eV. [b] Dirac-Fock results using ref 26. [c] Average over spin-orbit components. [d] Using the ECP from Table II and Gaussian basis set from Table I. [e] Gas phase; from ref 27 for Ag and Ag^+. [f] Optimized five configuration multiconfiguration SCF. The configurations are $5s^2$, $5s'^2$ (or $6s^2$), $6p_x{}^2$, $6p_y{}^2$, and $6p_z{}^2$, omitting the common 4d electrons. [g] From ref 28.

A molecular basis set for the SCF and CI calculations on the silver atom clusters was obtained as follows. Starting from an uncontracted $(3^s1^P5^d)$ fitted set of Gaussian functions to the respective numerical PVOs, we formed a contracted $[2^s1^P1^d]$ set by using the coefficients from a valence electron $[Kr](4d)^{10}(5s)^1$ (^2S) SCF calculation. The contracted s and p sets were then scale optimized in the Ag_2 diatomic molecule for the bond correlated (optimum double-configuration wave function) ground $^1\Sigma_g$ state at the fixed internuclear distance of 4.75 au. The resultant optimum p-type Gaussian exponent was found to be 0.1025. Since in these cluster studies the lowest energy electronic excited states were also sought, this p-type exponent was slightly increased in value and a diffuse p-type Gaussian added to the basis set. The final atom basis set used in all the calculations reported here is shown in Table II.

A comparison of atomic SCF energies in this basis is shown in Table III. It should be noted that in the ECP framework used here the 4d electrons are not incorporated into the frozen core. However, they are represented by only a minimal atomic orbital set of basis functions, which is not expected to have sufficient flexibility to accurately account for differential 4d electron relaxation effects in those electronic states of the silver atom clusters and their ions which are the result of electron excitation from the 4d subshell. Therefore, this study is restricted to the lower energy excited states of the silver clusters.

Preliminary calculations on Ag_2 showed that a more balanced description of the different diatomic states was obtained by carrying out the SCF calculations in $C_{\infty v}$ rather than $D_{\infty h}$ symmetry. The principle advantage of working in the lower symmetry lies in the enhanced ability to describe atomic polarization effects and is linked to the (localized) nonsymmetric dissociation limits

(18) A. Redondo, W. A. Goddard III, and T. C. McGill, *Phys. Rev. B: Solid State*, **15**, 5038 (1977).
(19) A. Zunger, *J. Vac. Sci. Technol.*, **16**, 1337 (1979).
(20) P. A. Christiansen, Y. S. Lee, and K. S. Pitzer, *J. Chem. Phys.*, **71**, 4445 (1979).
(21) H. Basch, *Symp.* Faraday *Soc.*, **No. 14**, 149 (1980).
(22) R. L. Martin and E. R. Davidson, *Mol. Phys.*, **35**, 1713 (1978).

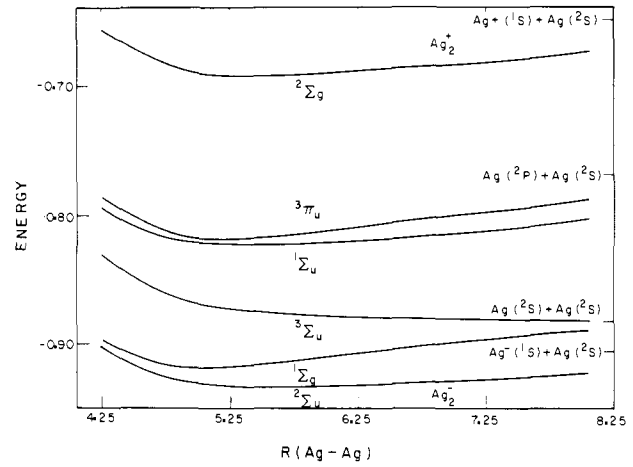

Figure 1. CI electronic state energy curves for Ag_2 and ions as a function of internuclear separation. Energy scale, in atomic units, is relative to −77 au.

Table IV. CI Calculated Spectroscopic Properties of Ag_2[a]

species	state	R_e, Å	ω_e, cm^{-1}	ΔE,[b] eV	D_e, eV
Ag_2^-	$^2\Sigma_u$	2.945	82	−0.45	0.80
Ag_2	$^1\Sigma_g$	2.681	131 (192)	0	0.94 (1.66)
	$^3\Sigma_u$			1.35	
	$^1\Sigma_u$	2.997	165 (155)	2.59 (2.85)	1.49 (2.55)
	$^3\Pi_u$	2.732	139	2.72	1.36
	$^1\Pi_u$	2.942	96	3.83	0.26
Ag_2^+	$^2\Sigma_g$	2.922	93	6.17	1.20

[a] Values in parentheses are experimental (gas-phase) values from ref 34 and 35. [b] Adiabatic excitation energy except for $^3\Sigma_u$ which is the vertical energy.

for certain of these states. When the core and 4d electrons are omitted, the homonuclear diatomic electronic states studied here arise from the $C_{\infty v}$-localized orbital configurations

Ag_2	$^1\Sigma_g$	$1\sigma^1 2\sigma^1$	$Ag(^2S) + Ag(^2S)$	(4)
	$^3\Sigma_u$	$1\sigma^1 2\sigma^1$	$Ag(^2S) + Ag(^2S)$	(5)
	$^1\Sigma_u$	$1\sigma^1 3\sigma^1$	$Ag(^2S) + Ag(^2P)$	(6)
	$^3\Pi_u$	$1\sigma^1 1\pi^1$	$Ag(^2S) + Ag(^2P)$	(7)
Ag_2^+	$^2\Sigma_g$	$1\sigma^1$	$Ag(^2S) + Ag^+(^1S)$	(8)
Ag_2^-	$^2\Sigma_u$	$1\sigma^2 2\sigma^1$	$Ag(^2S) + Ag^-(^1S)$	(9)

For the ground $^1\Sigma_g$ state a two-configuration SCF wave function of the form $A(1\sigma^2) + B(2\sigma^2)$ was used throughout. The $^1\Sigma_u$ energy curve was obtained from the CI calculation (to be described subsequently) by using the $^3\Pi_u$ SCF wave function. The CI energy curves for these states are shown in Figure 1 and the relevant calculated quantities are summarized in Table IV.

An explicit description of the potential energy surface effects and considerations in a homonuclear triatomic molecule for the specific case of the s-bonded Na_3 cluster has been given by Martin and Davidson.[22] Several interesting features arise out of the change in symmetry in going from the linear ($D_{\infty h}$) through the bent (C_{2v}) to the equilateral triangular (D_{3h}) conformation. A correlation diagram for the important valence MOs in Ag_3 is shown in Table V. Of particular importance is the degeneracy of the $5b_1$ and $7a_1$ molecular orbitals (MOs) at the equilateral triangle geometry. In C_{2v} symmetry the 5s atomic orbitals of the three Ag atoms comprise the $6a_1$, $5b_1$, and $7a_1$ MOs. On the basis of a simple symmetry orbital model (see subsequent discussion) the ground electronic state configuration of Ag_3, omitting the core and 4d electrons, is expected to be

$$6a_1^2\ 5b_1^1\quad ^2B_1 \tag{10}$$

which, however, in D_{3h} symmetry is degenerate with

$$6a_1^2\ 7a_1^1\quad ^2A_1 \tag{11}$$

as the $a_1'^2\ e'^1$, $^2E'$ state configuration. The degenerate state is formally Jahn–Teller unstable and is expected to distort away from D_{3h} symmetry in the directions of the a_1 and b_1 (e') skeletal vibrational modes. For convenience, therefore, all the SCF and CI calculations on Ag_3 were carried out in C_{2v} symmetry. Symmetry-breaking effects were observed in both the SCF molecular orbital and electronic state energies and even in the CI energies, for both the linear and equilateral triangle geometries. However, in all cases their magnitude was less than 0.1 eV. The experimental results with which the theoretical calculations are to be compared are generally taken from rare-gas matrix isolation studies. The low symmetry used here should then correspond to the local low-symmetry environments of the Ag clusters in the matrix, which are known to exist from the many observations of site splittings in such matrices.[23]

Table V. Correlation of Valence Orbitals among the Different Symmetries of Ag_3[a]

$D_{\infty h}$	C_{2v}	D_{3h}
$3\sigma_g$	$6a_1$	a_1'
$2\sigma_u$	$5b_1$	e'
$4\sigma_g$	$7a_1$	
$2\pi_u$	$4b_2$	a_2''
	$8a_1$	a_1'
$3\sigma_u$	$6b_1$	e'
$3\pi_u$	$9a_1$	
	$5b_2$	e''
$3\pi_g$	$4a_2$	
	$7b_1$	a_2'

[a] The serial numbering of the MOs includes the 4d electrons.

The lowest energy excited 5s → 5p states of the Ag_3 clusters arise from

$$6a_1^2\ 4b_2^1\quad ^2B_2 \tag{12}$$

$$6a_1^2\ 8a_1^1\quad ^2B_2 \tag{13}$$

$$6a_1^2\ 6b_1^1\quad ^2B_1 \tag{14}$$

$$6a_1^2\ 4a_2^1\quad ^2A_2 \tag{15}$$

where the $4b_2$, $8a_1$, $6b_1$, and $4a_2$ MOs are principally composed of Ag 5p orbitals. For Ag_3^-

$$6a_1^2\ 5b_1^2\quad ^1A_1 \tag{16}$$

and for Ag_3^+

$$6a_1^2\quad ^1A_1 \tag{17}$$

are expected to be the dominant electronic configurations describing the respective ground states of these species. Again, all these assignments are based on elemental MO concepts of level filling and the relationship between energy and orbital nodal patterns.

Direct SCF calculations were carried out on state configurations (10)–(12) and (15)–(17). All the virtual MOs for these state configurations were determined as eigenfunctions of the open-shell MO SCF operator (if there was one) which was defined by omitting the open-shell MO self-interaction term. Thus these improved virtual orbitals (IVOs)[24] should give a good representation of excited-state MOs. The energy dependencies of the valence MOs at a fixed Ag–Ag distance of 5.25 au as a function of bending angle from 0° (linear) to 65° (Ag_1–Ag_3–Ag_2 bond angle of 50°) are shown in Figure 2. In this figure each MO orbital energy is taken from the lowest energy SCF calculation in which that orbital is occupied. The higher MOs of each symmetry, which are not occupied in any SCF calculation, are taken as the IVOs from the respective SCF calculation having an occupied open shell of the same symmetry.

The CI calculations were carried out with the intention of correlating only the 5s and 5p electrons in the various states of Ag, Ag_2, and Ag_3, in order to obtain the 5s/5p part of the binding energy. The 4d electrons were therefore kept frozen as obtained in the parent SCF calculation, and the CI space also excluded

(23) T. Walker and T. P. Martin, *J. Chem. Phys.*, **70**, 5683 (1979).
(24) W. J. Hunt and W. A. Goddard III, *Chem. Phys. Lett.*, **3**, 414 (1969).

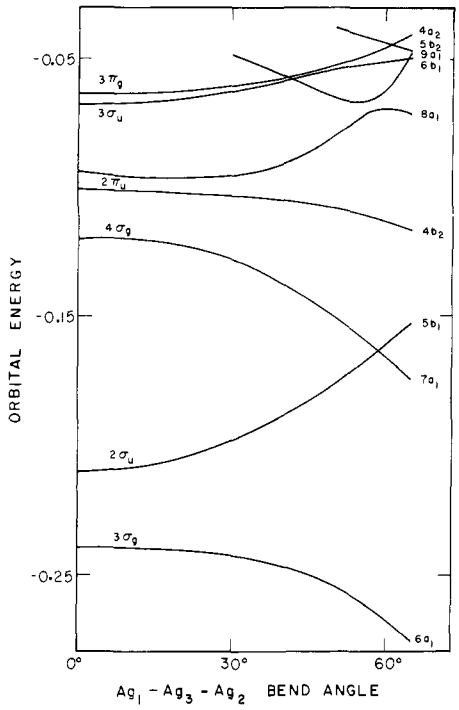

Figure 2. Energy dependence of the valence MOs of Ag_3 with bend angle at a fixed Ag–Ag bond distance of 5.25 au.

Table VI. Calculated Lower Energy VE-CI Electronic States of Ag_3[a]

species	state $D_{\infty h}$	C_{2v}	D_{3h}	relative to $^2B_1$: adiabatic	relative to $^2B_1$: vertical	relative to $^2A_1$: adiabatic	relative to $^2A_1$: vertical	equilibrium θ, deg
Ag_3^-	$^1\Sigma_g$	$^1A_1$	$^1A_1'$	−1.40	−1.08	−1.55	−0.39	0
	$^3\Sigma_u$	$^3B_1$	$^3A_2'$	−0.55	−0.27	−0.65	−0.65	58
Ag_3	$^2\Sigma_u$	$^2B_1$	^2E	0	0	−0.14	0.04	30
	$^2\Sigma_g$	$^2A_1$		0.14	1.08	0	0	60
	$^2\Sigma_g$	$^2A_1$	$^2A_1'$	1.81	1.82	1.67	1.97	32
	$^2\Pi_u$	$^2B_2$	$^2A_2''$	1.43	2.22	1.28	1.29	59
		$^2A_1$	$^2E'$	2.28	2.51	2.13	2.23	57
	$^2\Sigma_u$	$^2B_1$		2.32	2.67	2.22	2.22	55
	$^2\Pi_g$	$^2A_2$	$^2E''$	2.94	2.95	2.83	2.95	0
Ag_3^+	$^1\Sigma_g$	$^1A_1'$	$^1A_1'$	4.62	5.24	4.48	4.47	60

[a] Energies in eV.

the three $4d_{x^2+y^2+z^2}$ virtual MOs arising from the six Cartesian d-type basis functions. The CI wave functions thus include energy selected single- and double-electron excitation states of the 5s/5p electrons into the unoccupied spin-orbital space in all the orbital configurations that contribute significantly (CI expansion coefficient >0.1) to the electronic states of interest.[25] Electronic states of the same spin and symmetry were determined simultaneously in the same CI calculation by using the MOs of the lowest energy state of that spin and symmetry, with multiple parent reference configurations.

The final energy curves from the CI calculations are shown in Figure 3 and the spectroscopic data are summarized in Table VI. The unpaired spin populations for some states of Ag_3 are shown in Table VII.

Discussion

The comparison of electronic state energies for the silver atom, shown in Table III, gives some idea of the performance of the Table I basis set valence electron (VE) calculations compared with the spin–orbit averaged numerical all-electron (AE)[26] and experimental results.[27,28] Thus, the $^2S \rightarrow {}^2P$ transition energy is

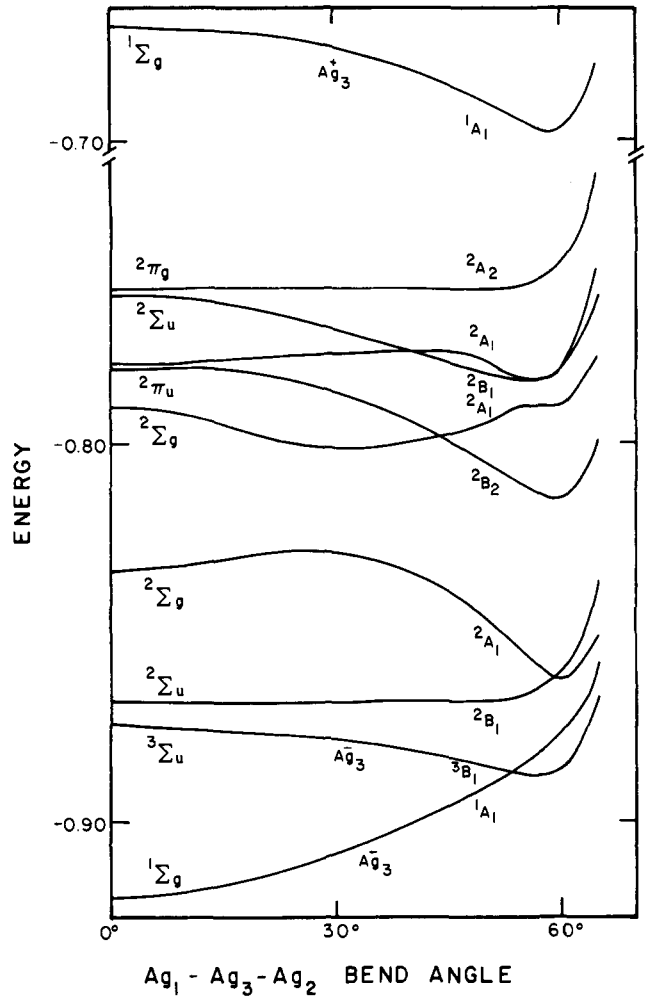

Figure 3. CI electronic state energy curves for Ag_3 and ions as a function of bend angle at a fixed Ag–Ag bond distance of 5.25 au. Energy scale, in atomic units, is relative to −116 au.

underestimated in the SCF (VE and AE) approximation by 0.6–0.7 eV compared to experiment. Likewise, the 5s ionization energy is (predictably) underestimated by ~1.2 eV. The VE-SCF electron affinity of atomic silver is calculated to be endothermic (unbound) by 0.12 eV. To evaluate the effect of electron correlation on this latter quantity a CI calculation (as described in the previous section) was carried out for the $5s^2$ pair of electrons. Both the CI and a 5 configuration VE multiconfiguration (MC) SCF calculation in the basis of Table I gave an electron affinity of −0.58 eV (bound). Since the experimental electron affinity of atomic Ag is −1.30 eV,[28] the VE calculated value is in error by 0.72 eV. Using a much larger atom basis, including sufficient flexibility to relax the 4d shell electrons, gave a VE-MCSCF electron affinity of −0.71 eV, in error by 0.59 eV. Within the relativistic ECP framework used here this latter value is then essentially the unrecovered correlation energy of the additional electron with the 4d electrons.

The optical absorption and emission spectra of the isolated Ag atom in rare-gas matrices at low temperatures have been studied extensively.[29-33] The $^2S \rightarrow {}^2P$ transition shows a pronounced energy shift with the nature of the matrix. For example, the $^2S_{1/2} \rightarrow {}^2P_{1/2}$ absorption band is identified at 3.71, 3.85, and 3.94 eV

(25) H. Basch, *J. Am. Chem. Soc.*, **97**, 6047 (1975).
(26) J. P. Desclaux, *Comput. Phys. Commun.*, **9**, 31 (1975).
(27) C. E. Moore, *Natl. Bur. Stand. (U.S.) Circ.*, **No. 467**, Vol. III (1971).
(28) H. Hotop, R. A. Bennett, and W. C. Lineburger, *J. Chem. Phys.*, **58**, 2373 (1973).
(29) F. Forstmann, D. M. Kolb, D. Lenthoff, and W. Schulze, *J. Chem. Phys.*, **66**, 2806 (1977).
(30) W. Schulze, H. U. Becker, and H. Abe, *Chem. Phys.*, **35**, 177 (1978).
(31) D. M. Gruen and J. K. Bates, *Inorg. Chem.*, **16**, 2450 (1977).
(32) G. Ozin and H. Huber, *Inorg. Chem.*, **17**, 155 (1978.
(33) H. Abe, W. Schulze, and D. M. Kolb, *Chem. Phys. Lett.*, **60**, 208 (1979).

Table VII. Total Charge and Unpaired Spin Populations in Ag_3[a]

configuration	θ, deg	state	total charge population[b]				unpaired spin population[b]			
			$5s_{1,2}$	$5p_{1,2}$	$5s_3$	$5p_3$	$5s_{1,2}$	$5p_{1,2}$	$5s_3$	$5p_3$
$6a_1^2 7a_1^1$	60	$^2A_1$	0.78	0.19	0.94	0.21	0.05	0.12	0.50	0.14
$6a_1^2 5b_1^1$	0	$^2B_1$	0.83	0.06	0.93	0.36	0.32	0.01	0	0.34
$6a_1^2 5b_1^1$	30	$^2B_1$	0.93	0.07	0.81	0.26	0.38	0.00	0	0.23

[a] From SCF calculations. [b] Sums of double-ζ contributions.

($T \rightarrow$ O K) in Xe, Kr, and Ar, respectively,[29] compared to 3.66 eV in the gas phase.[27] The increasing spectral blue shift with decreasing polarizability of the medium must be taken into account when ab initio (gas phase) calculated transition energies are compared with the optical spectra of matrix isolated dimers and clusters.

The electronic structural properties of Ag_2 are not well understood, and even the ground-state equilibrium bond distance (R_e) remains to be precisely determined, although a value of 2.469 Å has been estimated[34] from spectroscopic relationships in the Cu_2, Ag_2, and Au_2 series. A previous ab initio VE-CI study[21] using the same ECP but a larger (double-ζ) 4d orbital basis gave R_e = 2.62 Å, a dissociation energy (D_e) of 1.12 eV, and a harmonic stretch frequency (ω_e) of 242 cm^{-1} compared to R_e = 2.68 Å, D_e = 0.94 eV, and ω_e = 131 cm^{-1}, respectively, in Table IV. Thus the relaxation of the 4d orbitals accompanying molecule formation does influence to some extent the calculated spectroscopic properties, especially ω_e. The ground-state dissociation energy is reported to be 1.66 eV.[35] Thus the VE-CI method used here underestimates the diatomic binding energy and probably overestimates the bond distance somewhat. A recent nonrelativistic SW-Xα calculation[36] on Ag_2 predicts R_e = 2.84 Å and D_e = 1.56 eV while a hard-core valence bond model[37] gives R_e = 1.64 Å and D_e = 1.42 eV.

The adiabatic electron affinity of Ag_2 is calculated to be −0.45 eV which is smaller than the −0.58 eV obtained for the Ag atom at the same level of valence electron CI. Since $Ag_2^-(^2\Sigma_u)$ dissociates directly to Ag^- (^1S) + $Ag(^2S)$, a reasonable assumption is that both the unrecovered relaxation and correlation energy contributions of the core + 4d electrons to the electron affinity in Ag_2^- are very roughly the same as in Ag^- and certainly no larger. Thus it appears that the adiabatic electron affinity of Ag_2 is probably smaller than that of the Ag atom.

The calculated excited electronic states for Ag_2 shown in Table IV and Figure 1 have been restricted to those lying below 3 eV. The (spin–orbit averaged) lowest lying 4d → 5s excitation energy [$(4d)^{10}(5s)^1$ (^2S) → $(4d)^9(5s)^2(^2D)$] is experimentally found at 3.97 eV[27] in the gas phase, with the $^2D_{5/2}$ multiplet appearing at 3.79 eV, almost degenerate with the $^2P_{3/2}$ state. Thus the diabatic excited electronic states arising from 4d → 5s-type transitions in the clusters should start becoming important in that energy range. Clearly, as shown in Table III, the basis set used here cannot give a good description of these type excitations.

In the energy range for Ag_2 shown in Table IV the assigned $^1\Sigma_g \rightarrow {}^1\Sigma_u$ transition has been observed at 2.85 eV in the gas phase.[34-36] The calculated adiabatic excitation energy is 2.59 eV which shows that the VE-CI method used here also underestimates the 5s → 5s type transition energies, in this case by 0.26 eV. Low-temperature, rare-gas matrix isolation studies have located this transition at ~3.17 eV,[30,36] approximately independent of the rare gas. Thus the uniform matrix blue shift is in this case ~0.32 eV. The calculated vibrational stretch frequency for the excited state is in much better agreement with experiment than is found for the ground state. The "experimental" 2.55 eV dissociation energy for the $^1\Sigma_u$ state in Table IV is obtained by combining the experimental D_e of the $^1\Sigma_g$ (1.66 eV), the atomic $^2S \rightarrow {}^2P$ excitation energy (3.74 eV), and the $^1\Sigma_g \rightarrow {}^1\Sigma_u$ adiabatic transition energy (2.85 eV). The calculated $^1\Sigma_g$ and $^1\Sigma_u$ D_e's are thus seen to follow closely the observed trend in the experimental values.

The lowest energy $^1\Pi_u$ state, corresponding to the $1\sigma_g^1 1\pi_u^1$ state configuration, has also been assigned[8,32,36] to one or both of the gas-phase absorption bands observed at 4.44 or 4.66 eV.[34,35] Accordingly, the calculated $^1\Pi_u$ energy is underestimated by 0.6–0.8 eV. The corresponding absorption spectra in low-temperature rare-gas matrices show the usual blue shift as a function of rare gas for this essentially 5s → 5p-type transition.

The calculated ionization energy of Ag_2 is 6.17 eV (Table IV), compared with 6.43 eV calculated for the atom. Since Ag_2^+ dissociates to $Ag^+(^1S)$ + $Ag(^2S)$, it is reasonable to assume that the unrecovered relaxation and correlation energy errors for the ionized 5s electron are similar in Ag_2 and Ag. Thus the ionization energy is predicted to decrease in going from Ag to Ag_2, although formally the ionizing electron comes from a bonding orbital in Ag_2. This surprising trend comes about because the Ag_2^+ species is calculated to have a higher binding energy than ground-state Ag_2, a trend found also in the group 1a homonuclear diatomics Na_2 and K_2.[35] Experimentally, it has been reported that the dimer appearance potentials for each of the group 1b diatomics (Cu_2, Ag_2, and Au_2) is less than for the respective monomers.[38] This trend in ionization potentials has, of course, also been observed in Na_2 and K_2.[39]

In the calculations on the Ag_3 cluster no attempt was made to optimize the Ag–Ag bond distances due to the large uncertainties in the calculated value for Ag_2 and the relative shallowness of the potential curves as a function of the symmetric stretching mode. Instead, a fixed Ag–Ag distance of 5.25 au (2.778 Å) was chosen and the optimum bending angle found for each electronic state. The behavior of the lower valence MO SCF orbital energies in Ag_3 as a function of bend angle (Figure 2) follows what would be expected for these MOs on the basis of a qualitative MO picture. Thus the $6a_1$, $5b_1$, $7a_1$ (arising from the Ag 5s), and $4b_2$ (Ag 5p) MOs (in C_{2v} symmetry notation) are expected to have the following approximate analytic forms in the high symmetry cases

$$6a_1 \approx 5s_1 + 5s_2 + 5s_3$$

$$5b_1 \approx 5s_1 - 5s_2$$

$$7a_1 \approx 2(5s_3) - 5s_1 - 5s_2$$

$$4b_2 \approx 5p_{\perp 1} + 5p_{\perp 2} + 5p_{\perp 3}$$

where 1 and 2 are the terminal Ag atoms in the linear arrangement and $5p_\perp$ is the out-of-plane orbital. Thus the $6a_1$ MO is expected to be stabilized upon bending since an additional bonding phase interaction (Ag_1–Ag_2) is being added. On the other hand, the interaction between Ag_1 and Ag_2 in the $5b_1$ MO is antibonding and its energy should rise as those two atoms approach each other. As with the $6a_1$, both the $7a_1$ and $4b_2$ MOs should decrease in energy with bending because of the bonding phase interaction between Ag_1 and Ag_2.

The electronic state energies (Figure 3) as a function of bending angle generally mirror by above-outlined simple behavior of the MO orbital energies, complicated by substantial configuration interaction and avoided curve crossings in some cases. The lowest energy $^2B_1$ state [$6a_1^2 5b_1^1$] has electrons in MOs with opposing

(34) C. M. Brown and M. L. Ginter, *J. Mol. Spectrosc.*, **69**, 25 (1978).
(35) K. P. Huber and G. Hertzberg, "Constants of Diatomic Molecules", Van Nostrand: Princeton, NJ, 1979.
(36) G. A. Ozin, H. Huber, D. McIntosh, S. Mitchell, J. G. Norman, Jr., and L. Noodlemann, *J. Am. Chem. Soc.*, **101**, 3504 (1979).
(37) J. C. A. Boeijens and R. H. Lemmer, *J. Chem. Soc. Faraday Trans. 2*, **73**, 321 (1977).
(38) P. Schissel, *J. Chem. Phys.*, **26**, 1276 (1957).
(39) A. Herrmann, E. Schumacker, and L. Woste, *J. Chem. Phys.*, **68**, 2327 (1978).

orbital energy dependencies as a function of bend angle (θ). The result (Table VI) is an extremely shallow minimum at $\theta \approx 30°$, reflecting the stronger rise of the $5b_1$ orbital energy with increasing θ. Removing the $5b_1$ electron then naturally gives an equilateral triangular ($^1A_1'$) Ag_3^+ ground-state geometry. On the other hand, adding an electron to Ag_3 to form Ag_3^- [$6a_1^2 5b_1^2$] logically gives a linear ground-state ($^1A_{1g}$) anion, although the $6a_1^2\ 7a_1^2$ configuration becomes dominant at high ($\theta \approx 60°$) bend angles. The peculiar shape of the lowest $^2A_1$ state of Ag_3 is the result of the avoided crossing of two diabatic $^2A_1$ configurations: $6a_1^1 5b_1^2$, which is more stable at low bending angles, and $6a_1^2 7a_1^1$, which falls below it in energy at large θ. The resultant avoided crossing can almost be predicted from the relative behaviors of the $5b_1$ and $7a_1$ MOs as a function of θ (Figure 2): the former more stable below $\theta \approx 60°$ and the latter falling below it at higher bend angles. Analogously, the first $^2B_2$ state of Ag_3[$6a_1^2 4b_2^1$] is found (Table VI) to be triangular.

The adiabatic electron affinity of Ag_3 is VE–CI calculated to be −1.40 eV (Table VI). This value is quite a jump from the electron affinities calculated for Ag and Ag_2 of −0.58 and −0.45 eV, respectively. The lowest energy dissociation path for linear ($^1\Sigma_g$) Ag_3^- [$6a_1^2 5b_1^2 = 3\sigma_g^2 2\sigma_u^2$ (linear)] to $Ag_2(^1\Sigma_g)$ + $Ag^-(^1S)$, which is calculated here to be 1.01 eV endothermic, involves an avoided electronic state curve crossing corresponding to an orbital crossing of the $2\sigma_u$ and $4\sigma_g$ MOs with increasing Ag_1–Ag_3 distance. It is therefore difficult to relate the unrecovered relaxation and correlation energy contributions to the electron affinity in the Ag_3^- ion cluster to those in the dissociation fragments; but a reasonable assumption is that it is not much smaller in Ag_3^- than in the fragments. The experimental value of the Ag_3 cluster electron affinity should then be close to −2.0 eV, similar to that calculated by Baetzold.[6] The electron affinity of Ag_3 is sufficiently large to accommodate at least one [the $^3B_1$ state in Table VI and Figure 3, which dissociates to $Ag_2^-(^2\Sigma_u)$ + $Ag(^2S)$] and possibly more excited Ag_3^- states which are bound relative to ground-state Ag_3 plus a free electron. Figure 3 shows that the $^3B_1$ state is triangular.

As noted above, the electron affinity in the series Ag_n, n = 1–3, is calculated to decrease and then increase in value. Such a saw-tooth trend has been observed in the mass spectral intensity distribution of secondary ion mass spectrometry experiments detecting negatively charged silver atom clusters,[40] where it is found that the anions with an odd number of atoms are relatively abundant. This odd/even intensity oscillation has been interpreted as an indication of the special stability of clusters with an odd number of silver atoms.[6,32,40] Baetzold[6] has further identified this alternating stability with the greater (lesser) stability of closed (open) shell Ag atom cluster systems.

The adiabatic ionization potential for Ag_3 is VE-CI calculated to be 4.62 eV (Table VI), significantly smaller than the 6.17 and 6.43 eV calculated for Ag_2 and Ag, respectively. Here again, the unrecovered relaxation and correlation energy contributions of the core and 4d electrons to the Ag_3 ionization energy are expected to be smaller than in Ag_2, increasing somewhat the VE-CI calculated difference in ionization potentials between Ag_2 and Ag_3. Here, the mirror-image odd/even alternation effect in the electron affinities is noted,[6,32] with clusters consisting of an odd number of atoms having the lowest ionization energies. The same trend has been observed in the Na_n and K_n series.[39] The adiabatic dissociation energy for the process Ag_3^+ ($^1A_1$) → Ag_2^+ ($^2\Sigma_g$) + $Ag(^2S)$ is calculated to be 0.97 eV.

A fundamental question about Ag_3 that needs to be answered is the geometry and nature of its electronic ground state. The posed question is complicated by the fact that the calculations are appropriate to a gas-phase molecule while almost all the experimental data on Ag_3 relate to the low-temperature, rare-gas matrix-isolated species. With this reservation in mind, it can be seen from Table VI and Figure 3 that there are two possible candidates for the ground electronic state: a linear or weakly bent $^2B_1$ state or a very bent (triangular) $^2A_1$ state with a calculated adiabatic energy difference of only 0.14 eV between them, favoring the former. This separation energy is probably too small a value upon which, by itself, to predict the ground electronic state and geometry because both the approximations inherent to the calculations and the matrix energy effects can each lead to differences as large as several tenths of an electron volt in magnitude. One way of deciding between the $^2B_1$ and $^2A_1$ ground states is by comparing their calculated spectroscopic properties with the calculated values. This is the approach taken here and discussed below.

In the Raman spectrum study of Schulze et al.[41] on matrix-isolated Ag_3 only a single Raman band was observed at 120.5 cm^{-1} and assigned to the symmetric stretch frequency of a linear geometry Ag_3. For either a C_{2v} or D_{3h} symmetry triatomic species more than one vibrational mode is Raman active, whereas only one Raman active band is expected for a linear ($D_{\infty h}$) triatomic. This conclusion about the geometry of ground-state Ag_3 has recently been questioned[42] on the grounds that for moderate bend angles the asymmetric stretch would be too weak to be observed and that a very low-frequency bending mode would have been out of the range of detection in the matrix Raman study. The $^2B_1$ state is here calculated (Table VI) to be nearly linear with a very shallow minimum at $\theta \approx 30°$. The VE-CI energy difference between $\theta = 10°$ or $\theta = 50°$ and $\theta = 30°$ is only ~0.01 eV in both cases. Within the resolution of these calculations such an energy difference is insignificant, although it is also found in the VE-SCF calculations where the equilibrium bond angle is larger ($\theta \approx 45°$) and the energy minimum deeper (energy difference between $\theta = 30°$ and $\theta = 50°$ is ~0.03 eV). Thus, a slightly bent $^2B_1$ state with a very shallow potential minimum as shown in Figure 3 clearly satisfies both the above enumerated reasons for the observation of only one band in the matrix Raman spectrum of Ag_3. On the other hand, for the $^2A_1$ state, which is predicted to have a very bent triangular geometry, two Raman active modes should have been observed. Thus, if the assignment of the Raman spectrum to Ag_3 is correct,[41,43] the choice of a linear or slightly bent $^2B_1$ ground state for Ag_3 is indicated.

Ozin and Huber[43] have recently reported that "ESR observations for argon entrapped photogenerated Ag_3 showed large hyperfine couplings of the unpaired electron to two equivalent silver atoms ... consistent with the idea of a mainly 5s localized electron in either a linear or bent Ag_3 molecule." As is clear from Table VII, the $^2A_1$ [$6a_1^2\ 7a_1^1$] state configuration of Ag_3 has almost no unpaired 5s spin population on the terminal silver atoms and almost all the unpaired 5s spin population in the $7a_1$ MO is concentrated on the apical silver atom. On the other hand, the $^2B_1$ [$6a_1^2\ 5b_1^1$] state configuration, with the unpaired spin in the $5b_1$ MO, which allows only zero unpaired 5s population on the apical (or middle) Ag atom, fits the description quoted above. For convenience, the VE-SCF results have been quoted here rather than the VE-CI results. However, for each of these electronic states in their respective equilibrium geometries the single configuration SCF wave functions have CI coefficients of ~0.96, which makes them the overwhelmingly dominant configuration in the CI expansion. Thus, again, a comparison of these calculations with the reported experimental results indicates that the ground electronic state of Ag_3 is a linear or mildly bent $^2B_1$ state.

It is relevant at this point to compare the results obtained here for Ag_3 with those obtained in a similar study on Na_3.[22] Interestingly enough, the topological features of the ground potential surfaces of Ag_3 and Na_3 are very similar both in shape and energy, in line with the valence isoelectronic structure of Ag and Na. For example, the ground dissociation energy of Ag_3 according to $Ag_3(^2B_1)$ → $Ag_2(^1\Sigma_g)$ + $Ag(^2S)$ is VE-CI calculated to be 0.22 eV compared to 0.37 eV calculated for Na_3.[22] The accuracy of the Ag_3 value is not clear since the ground dissociated fragments do not correlate with the $^2B_1$ but rather with the $^2A_1$ state. One notable difference between the two studies was the simultaneous

(40) G. Hortig and M. Muller, *Z. Phys.*, **221**, 119 (1969).

(41) W. Schulze, H. U. Becker, R. Minkwitz, and K. Manzel, *Chem. Phys. Lett.*, **55**, 59 (1978).

(42) M. Moskowitz and D. P. Di Lella, *J. Chem. Phys.*, **72**, 2267 (1980).

(43) G. A. Ozin and H. Huber, *Inorg. Chem.*, **18**, 1402 (1979).

optimization of the atom–atom bond distances with bend angle in the Na_3 work. Thus the ground $^2B_1$ state is found to be more bent in the latter study with a 0.13-eV energy difference between the equilibrium bent form and the linear geometry. The $^2A_1$ state is also found to be more bent ($\theta > 60°$) with only a 0.03-eV adiabatic separation energy from the $^2B_1$ state. The striking similarity between the matrix-isolated optical absorption spectra of Ag_n and Na_n ($n = 1$–4) has already been noted.[43] Since relaxation and correlation effects involving the Ag 4d electrons have not been adequately taken into account here, the precise validity of this comparison with regard to the ground-state electronic structure description of Ag_n remains to be further investigated.

As mentioned before, the matrix isolation spectra of atomic silver and its clusters show clear evidence of matrix site perturbatons and even, perhaps, multiple trapping sites.[44] In addition, Ozin et al.[45] have recently reported that photoexcitation of Ag_3 entrapped in argon gives different optical absorption and emission spectral characteristics than photoexcited Ag_3 in Kr or Xe. The behavior of the Kr/Xe matrix spectra has been interpreted as indicating a geometrical isomerization of ground-state Ag_3 via a radiationless decay process. On the basis of Figure 3 and Table VI this proposal corresponds to the process

$$Ag_3[6a_1^2\ 5b_1^1, {}^2B_1] \xrightarrow{h\nu} Ag_3^* \rightarrow Ag_3[6a_1^2\ 7a_1^1, {}^2A_1]$$

Ag_3/Ar, on the other hand, is found to photodissociate under the same conditions. One possible explanation for the different behavior of Ag_3/Ar is that the Ag_3 is trapped originally in the large bend angle $^2A_1$ state and the process is

$$Ag_3[6a_1^2\ 7a_1^1, {}^2A_1] \xrightarrow{h\nu} Ag_3^* \rightarrow Ag_2(^1\Sigma_g) + Ag(^2P)$$

Clearly, the Ag_3* excited states in these two cases need not be the same.

Two sets of bands observed in the low-temperature, matrix-isolated optical absorption spectra of deposited silver have been assigned to Ag_3.[8,9,30,32,45,46] A correlation of the peak positions between gas-phase and rare-gas matrix spectra has been sketched by Schultze and Abe.[8] In summary, a long wavelength band is observed at a gas-phase extrapolated energy of 2.55 eV and a short wave length triplet straddles the 4.5–4.9-eV energy range.

As can be seen from Table VI and Figure 3, the calculated density of states in the energy region shown is relatively high, as opposed to the identification experimentally of only one low-energy absorption with the Ag_3 cluster. Oscillator strengths have not been calculated here for the electronic transitions. It was felt that they would be of insufficient accuracy upon which to base assignments due to the approximate nature of the calculations and the large amount of strongly bend angle dependent configuration mixing found for the manifold of $^2A_1$ states. However, some idea of the origin of the long wavelength band in Ag_3 and the nature of the terminating excited state can possibly be obtained by considering the symmetries and shapes of the calculated states shown in Table VI and Figure 3.

A vertical excitation from the bent ($\theta \approx 30°$) $^2B_1$ ground state of Ag_3 reaches the first excited state, the $^2A_1$ Jahn–Teller partner (at $\theta = 60°$) of the ground state, at 1.08-eV higher energy. Martin and Davidson[22] calculate a very small oscillator strength for the analogous transition in Na_3. The next calculated excited state is also a $^2A_1$ at 1.82 eV from the ground state. As described previously, these two $^2A_1$ states have an avoided state crossing due to the crossing of the $6a_1^1\ 5b_1^2$ and $6a_1^2\ 7a_1^1$ single-configuration energies. In the neighborhood of $\theta \approx 30°$, then, excitations to these two $^2A_1$ states from the $6a_1^2\ 5b_1^1$, $^2B_1$ ground state corresponds to a mixture of the $6a_1 \rightarrow 5b_1$ and $5b_1 \rightarrow 7a_1$ one-electron transitions, both of which are of the 5s → 5s-type. The next three calculated excited states ($^2B_2$, $^2A_1$, and $^2B_1$ at 2.22, 2.51, and 2.67 eV, respectivley) are electic dipole forbidden from the ground state in the linear geometry as u ↔ u transitions, although only the $^2B_2$ state is forbidden also in C_{2v} symmetry. Thus, a likely candidate for the observed 2.55-eV absorption band in Ag_3 is to the second $^2A_1$ state calculated at 1.82 eV above the ground state. This assignment is consistent with the underestimation of the calculated excitation energy, as found in atomic Ag and Ag_2.

The vertical electronic excitations from a triangular ($\theta \approx 60°$) $^2A_1$ [$6a_1^2\ 7a_1^1$] state, as shown in Figure 3, would be expected to give a different looking optical absorption spectrum from the $^2B_1$ ground-state spectrum, although nothing definitive can be predicted without more accurate calculations. The first excited state at $\theta \approx 60°$ is the $^2B_2$ ($^2A_2''$ in D_{3h} symmetry) which is electric dipole forbidden from a pure e state, although not from $^2A_1$. The next excited state is the $^2A_1$ at 1.97 eV (or 1.67 eV adiabatic) whose orbital configuration character (at $\theta = 60°$) is mainly $6a_1^2\ 8a_1^1$. The lowest energy vertical $^2A_1 \rightarrow {}^2A_1$ transition corresponds mainly to the one-electron $7a_1 \rightarrow 8a_1$ promotion which is a 5s → 5p-type transition, in contrast to the corresponding lowest energy $^2B_1 \rightarrow {}^2A_1$ vertical excitations which, as noted above, are mainly of the 5s → 5s-type.

Conclusions

The behavior of the lower valence MO SCF orbital energies in Ag_3, as a function of bend angle, follows what would be expected for these MOs on the basis of a simple symmetry orbital model and the relationship between energy and orbital nodal patterns. The electronic state configuration energies generally conform to the additive behavior of the occupied orbital energies, complicated by substantial configuration interaction and avoided curve crossings. In these respects there is a great similarly between Ag_3 and Na_3.

Ag_3^+ is predicted to have an equilateral triangular geometry, and a significantly lower ionization potential is calculated for Ag_3 than for Ag_2. On the other hand, Ag_3^- is found to be substantially bound (relative to Ag_3 + an electron) and linear in geometry. The mirror-image, saw-tooth behavior of the electron affinities and ionization potentials of larger silver atom clusters with size, noted in the semiempirical MO calculations of Baetzold,[6] is also found here.

The ground electronic state of Ag_3 ($^2B_1$) is predicted to be slightly bent with a very shallow bending mode potential surface. In the neighborhood of the equilateral triangular geometry an $^2A_1$ state becomes the ground state, lying only 0.14 eV above the $^2B_1$ state. The $^2A_1$ and $^2B_1$ states are two branches of a Jahn–Teller split degenerate $^2E'$ state at D_{3h} symmetry. The closeness in energy of these two states could lead to the geometrical isomerization effects discussed by Ozin et al.[45] on the basis of low-temperature, rare-gas matrix isolation spectra of Ag_3.

Acknowledgment. This work was supported, in part, by a grant from the U.S. Israel Binational Science Foundation, Jerusalem, Israel.

(44) G. A. Ozin, *J. Am. Chem. Soc.*, **102**, 3301 (1980).
(45) G. A. Ozin, H. Huber, and S. A. Mitchell, *Inorg. Chem.*, **18**, 2932 (1979).
(46) S. A. Mitchell and G. A. Ozin, *J. Am. Chem. Soc.*, **100**, 6776 (1978).